Δελτίο Ελληνικής Γεωλογικής Ετοιρίας τομ. XXXV, 118 - 128, 2003
Bulletin of the Geological Society of Greece vol. XXXV, 118 - 128, 2003

Surface Displacement Model of Nisyros Volcanic Field deduced from DInSAR Analysis & DGPS Measurements

V. SAKKAS[1], E. LAGIOS[1], IS. PARCHARIDIS[1] and SP. VASSILOPOULOU[1]

ABSTRACT

Combined DGPS measurements and Differential Interferometry (DInSAR) were applied on Nisyros Volcano to study the ground deformation of the area. The GPS network was established to monitor the crustal deformation in June 1997, after an intense local seismic activity, which broke out in 1996.

A general uplift was measured at all stations of the network ranging from 14 to 140 mm, which after 1998 showed a decline, maintaining though the uplifted character of the deformation. The amplitude of the horizontal deformation was ranging from 13mm to 40mm for the period of only three months (June-Sept. 1997), which increased up to 53mm for the next eight months. The directions of the horizontal deformation observed at the GPS stations (1997-2001) indicate that the island is generally expanding mainly to the East, West and South. Detailed modelling attempts of the observed DGPS displacements from 1997-2001 were made. Least squares detailed modelling applying an elastically expanding source (Mogi Model) at a depth of 7000m, and at approximately the centre of the island, seems to generally fit and explain the observed deformation (1997-2001), both in the vertical and horizontal dimension. Combined modelling including the Mogi source and modelling displacements along/across local faults at the NW and NE part of the island was proved particularly effective in an attempt to better fit the observed DGPS values.

Differential SAR Interferometric (DInSAR) analysis using pair images between 1995, 1996, 1999 and 2000 confirmed the deformation observed by the DGPS measurements. The calculated location of the Mogi source representing the pressure changes in the magma chamber is consistent to earlier Audio-Magnetotelluric investigations of the high enthalpy geothermal field of Nisyros, detecting a conductive (magmatic) body at relatively upper crustal layers. At similar depths, a low velocity zone interpreted as magma chamber(s) is also identified by detailed tomographic seismic studies.

1. Introduction

The eastern sector of the Hellenic Volcanic Arc (HVA) including the islands of Kos, Yali and Nisyros, (Fig. 1) seems to be geodynamically very active, since it comprises the largest volumes of volcanic products, which were emitted during the past 160,000 years forming a caldera of 15-20 km, and it is at present a region of high tectonic unrest (Jackson. 1994).

The island of Nisyros (Fig. 2) is a strato-volcano with a large central caldera (Papanikolaou & Lekkas 1990; Vougioukalakis 1993). The volcano was raised up above sea level about 66,000 years ago and may have risen as high as 1000 meters 24,000 years ago. The main central cone of the volcano collapsed during a plinian eruption of dacite pumice, to leave the caldera. After the caldera formed, eruptions produced the lava domes. Pumice from this eruption may be found in 100m thick beds on the higher parts of the island. The base of the island is made of hyaloclastite, lava flows, and breccias, mostly of andesite composition. Pyro-

[1] *Space Applications in Geosciences, Laboratory of Geophysics, University of Athens, Panepistimiopolis, Ilissia, Athens 157 84, Greece.*

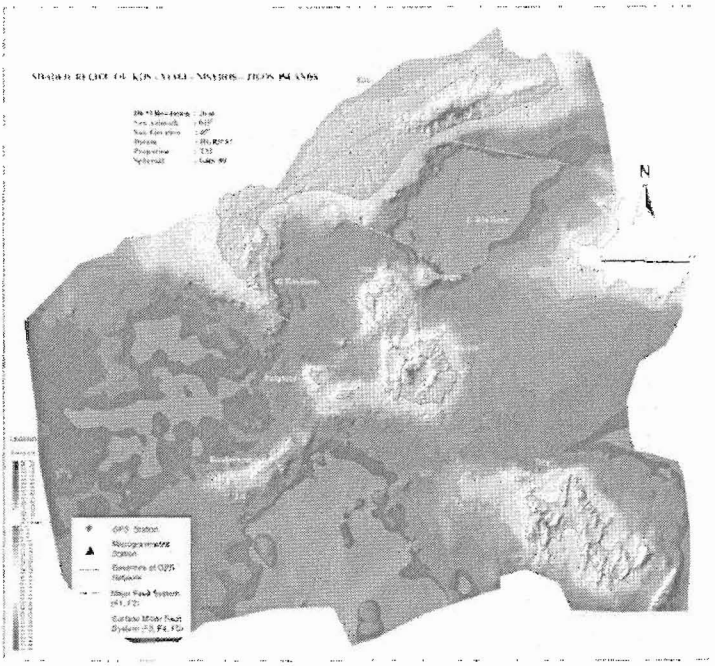

Figure 1. Bathymetry and Topography of broader study area (GEOWARN IST-1999-12310 project).

clastic deposits and volcanic domes of dacite composition cap these rocks. The pyroclastic deposits are related to two explosive phases of the volcano.

Tectonically, Nisyros Island (Fig. 2) is characterized by a series of NE-SW trending fault system, a NW-SE trending fault system and E-W and N-S faulting systems, as well as the Caldera Rim. The results are in accordance with previous structural and geological investigations (Papanikolaou et al. 1991; Vougioukalakis 1993).

Although the last volcanic activity on Nisyros dates back at least 15,000 to 20,000 years, the present geodynamic activity encompasses high seismic unrest, widespread fumarolic activity, and numerous hot springs close to the sea level all around the island (Fig. 2). Violent earthquakes and steam blasts accompanied the most recent hydrothermal eruptions in 1871-1873 and 1887 (Gorceix 1873 a,b,c). Mudflows and hydrothermal vapours rich in CO_2 and H_2S were emitted from fracture zones, which cut the caldera of the volcano and extend towards NNW through the vicinity of Mandraki into the island of Yali and even towards Kos. This feature indicates the existence of deep reaching zones of crustal weakness, which will probably act as zones of ascent of magma-batches coming from the upper mantle and lower crust, upon volcanic unrest.

The most recent seismic activity started early 1995 with earthquake magnitudes between M=4 R and M=5 R, which in July 1996 damaged about 30 houses in Mandraki. From June to September 1997, high-seismic activity (earthquakes up to M=5.5R and with hypocenters down to about 10 km depth) occurred again on Nisyros, and was accompanied by increased tectonic and fumarolic activity along the western edge of the hydrothermal crater field.

There are three primary sources of crustal deformation at volcanoes: (i) pressure changes in high-level magma storage areas and conduits, (ii) magmatic intrusions and (iii) earthquakes. The most common model to interpret crustal deforma-

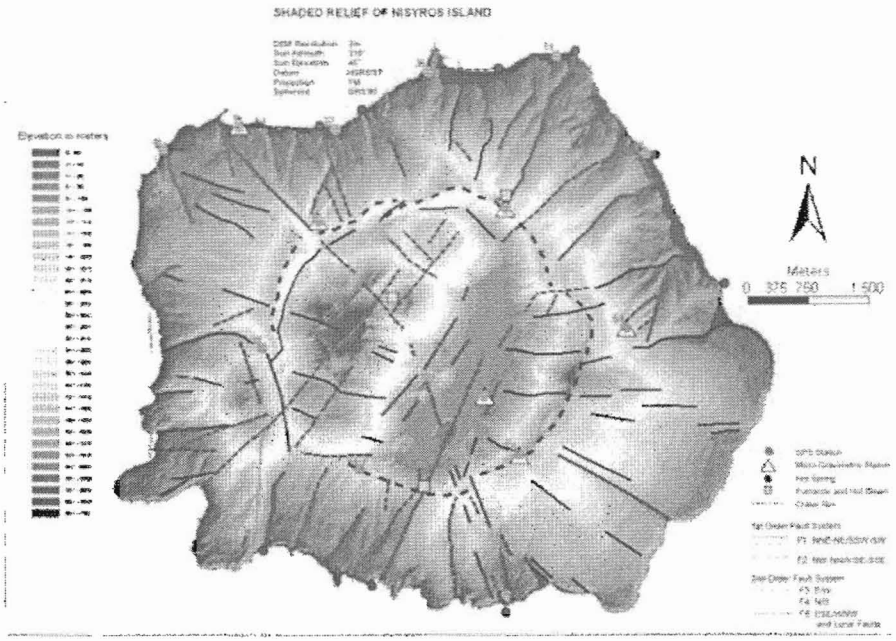

Figure 2. Topography of Nisyros Island showing the main tectonic features. The GPS stations are marked with blue circles.

tion caused by pressure changes in high-level magma chambers is the Mogi model (Mogi 1958). Deformation associated with earthquakes and dyke intrusions is not to be calculated using the Mogi model. For such deformation Okada (1985) presented a model, which can easily implemented in a computer.

There is a number of different geodetic techniques to monitor crustal deformation with different results of accuracy. In the last decade, Differential GPS (DGPS) measurements and Synthetic Aperture Radar (SAR) Interferometry has been proven to be a powerful technique for the monitoring of small surface changes on large-scale areas (Zebker & Goldstein 1986). Differential Interferometry (DInSAR) is the most interesting technique of SAR Interferometry in the two-dimensional mapping of deformation with very high accuracy (mm to cm level). Both techniques allow the study of a wide range of surface deformations.

2. Differential Global Positioning System (DGPS) Measurements

The DGPS network (Fig. 2) was established at Nisyros in June 1997 (Lagios et al. 1998). Measurements were undertaken in September and December 1997, twice in 1998, and annually since 1999 onwards. A station at the NE part of Kos (Fig. 1) was chosen as reference station (with fixed coordinates) of the network. Geodetic receivers of WILD type (SR 299 and SR399) were used for the field GPS campaigns.

The Nisyros GPS network consists of 16 stations covering whole of the island. Since the dimensions of the network are relatively small, being controlled by the relatively small dimensions of Nisyros (about 8 km diameter), it is evident that the length of the measured baselines between the GPS stations in Nisyros is considerably small (3-4 km). The larger length baseline is 32 km, from the Kos reference station to Nisyros.

In-situ processing and adjustment of the GPS

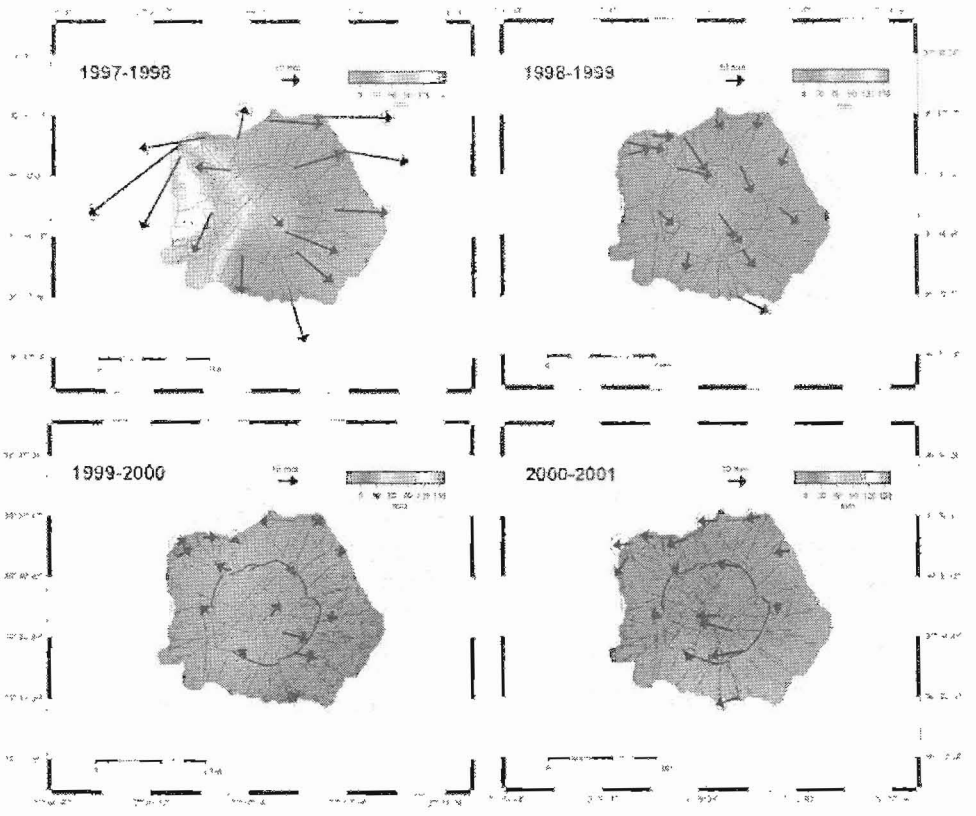

Figure 3. Annual display of the DGPS results. The Horizontal deformation is represented by arrows, while the vertical displacement is presented by colour contouring (scale in upper right corners).

observations were made using the GPS post-processing Static Kinematic Software (S.KI. Pro, Version 3.2, 1999) of Leica, which was adequate due to (i) the small distances of the measured baselines and (ii) the very high rate and long-time recording (Lagios, 2000). Post processing of the GPS observations were made using the *Bernese GPS Software Version 4.2* (2001) (Rothacher et al., 1993), and increased the accuracy of the GPS network, especially on the longest baseline between Kos and Nisyros. The calculated uncertainty is typically 2-3mm in the horizontal component, and twice that value in the vertical component. The adjusted values for the observational periods were considered for the detection of the ground deformation.

A consecutive annual overlook of the GPS results during the whole period of the re-measurements can give a qualitive and quantitive image of the ground deformation in Nisyros (Fig. 3). It appears that the maximum of the horizontal displacement took place during the period 1997-1998, while the seismic activity was still in progress. The amplitude of the horizontal deformation was ranging from 20 mm to 60 mm. In the following period 1998-1999, there was a decline in the horizontal deformation, ranging from 10-20 mm, and even less in the period 1999-2000, of about 10 mm. However, in the period 2000-2001, it seems that the deformation attained larger values, of about 15 mm, at some GPS stations.

Concerning the vertical displacement, it is

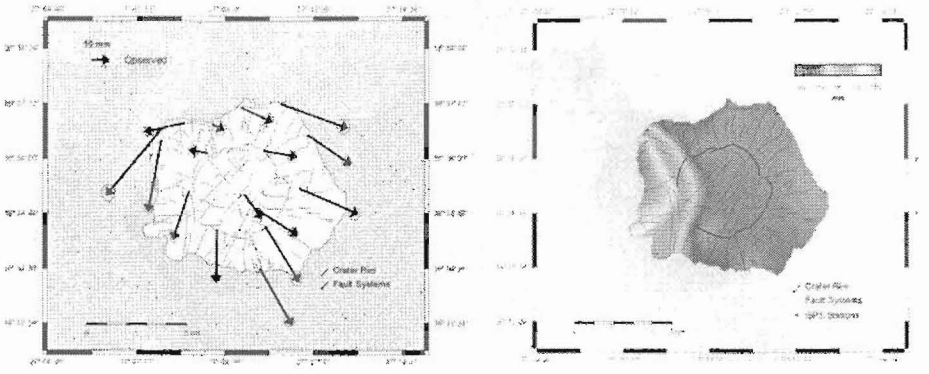

Figure 4. Observed horizontal (left part) and height (right part) displacements on Nisyros deduced from DGPS measurements for the period 1997-2001.

obvious that there was a general uplift of the whole island during the period of the re-measurements. The largest vertical changes took place in the period of 1997-1998 of amplitude of 40-60 mm in the larger part of the island, while at three stations at the NW part, the amplitude was reaching values 60 and 140 mm. These stations are located at the uplifted side of the re-activated fault that crosses Mandraki and caused severe damages in 1996 (Ioannides, 1998). In the following period 1998-1999, the uplift continued by only 8 mm. In the period 1999–2000, it appears that there was a deflation by 15 mm, while a further uplift of about 10 mm was again noticed in 2000-2001.

Figure 4 presents the overall deformation observed in Nisyros for the whole period of the measurements 1997-2001. A total horizontal displacement of 10-60 mm and vertical displacement, representing an uplift of the ground surface, ranging from 30-140 mm can be seen.

It appears that the island is apparently "opening up" along the two major faulting zones F1 and F2 (Fig. 2). The motion of the GPS stations at the half NE part of the island is almost ESE, turning progressively to the SE at its southern part. At the half western part, the direction of deformation is clearly to the SW, with the exception of a couple of stations near the NE part of Nisyros, which show a motion to the NE and WNW, respectively.

2.1 Modelling – Interpretation

In active volcano environments, the cause of deformation is usually linked to magma extraction and replenishment of a magma reservoir. Thus it can be seen as magma chamber inflation/deflation processes. In such cases the application of an "elastically expanded point source" (Mogi 1958) usually explains the observed deformation (Sigmundsson et al. 1992). For the case of Nisyros, the "Mogi model" has also been applied in an attempt to model and explain the deformational features observed on Nisyros by DGPS measurements.

Theoretical relative displacements were calculated from the GPS points at varying depths and locations beneath the centre of the island. The residual of the observed (1997-2001) and theoretical displacements is minimised in the sense of least-squares to find the best fit. The best fitting source was finally located at a point with the coordinates [36° 35' 43.24'' N, 27° 9' 34.28'' E (in WGS'84) or 4054334 (±500)m N, 782498 (±500)m E (in the Hellenic datum HGRS'87)] (see red point in Figure 5) at a depth of 7000 ± 1000 m, and 75m of the radius of the "expanding sphere" associated with the "source strength parameter" (Sigmundsson, 1995) of the Mogi model. It was found that the calculated Mogi displacements for the horizontal component (Fig. 5, red arrows) seemed to generally fit the observed ones (black

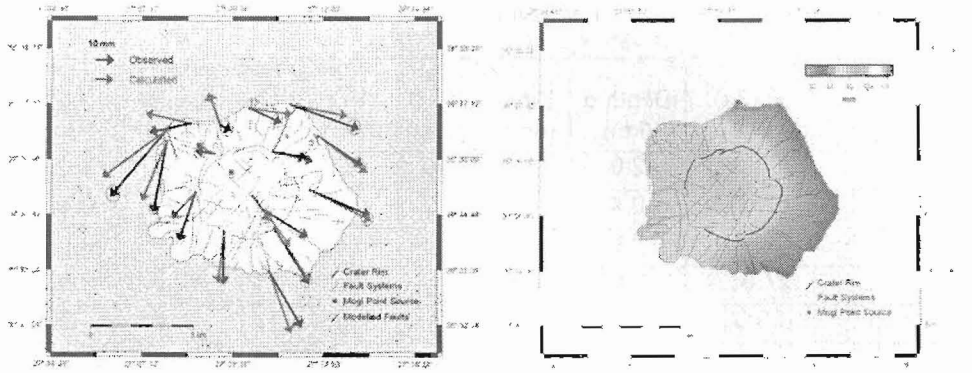

Figure 5. Combined calculated (Mogi Model & Fault Modelling) displacements for the period 1997-2001. The red dot (left image) indicates the location of the Mogi point source. Modelled faults are marked in red.

arrows, Fig. 5).

There is an exception though at the NW and the NE part of Nisyros, where a discrepancy between the observed horizontal DGPS component and the theoretical Mogi arrows is noticed. The Mogi (red) arrows are expected to point radially outwards from the Mogi source at those regions. That would suggest that the deformation at those parts of the island for the period 1997-2001 is not only controlled by an elastically expanded point-source (change of pressure in magma chamber), but also other factors should be taken into consideration. Additional controlling parameters of the deformation patterns at those areas must be taken into consideration, such as motions along nearby reactivated faults. The presence of these faults and its possible reactivation by the change of the stress field may differentiate not only the direction of the observed displacements, but also may change the amplitude of motion with respect to the calculated Mogi model. Such case was already marked at the NW part of Nisyros in the 1996 seismic crisis, when an older fault was activated passing through the town of Mandraki, causing damages in the houses by its distinct observed displacements (Ioannides, 1998).

For that reason modelling along faults at the NW and NE part of the island was also made applying the algorithm developed by Feigl and Dupre (1999). The combined result, including the above Mogi point source and the detailed modelling at a number of five (5) faults, is outlined in Figure 5, representing the horizontal deformation. The values of the various parameters required for the modelling, is shown in Table 1. The modelled parameters are outlined in Figure 6.

The activation of the F2 fault system, namely the fault No 1 (Table 1, Fig.5) (with direction from SSE to NNW and extending into the sea, reaching the Yiali coast to the north) passing through Mandraki (Ioannides, 1998) can justify the fault modelling in the NW part of Nisyros. However, similar faulting activity at the NE part of the island is not reported, even thought it cannot be excluded, since most attention in the 1996-97 seismic crisis was mainly concentrated on the populated NW part of the island (Mandraki), where the house damages took place. The Fault modelling (Fig. 5, red arrows) at the NE part presents only a possible interpretational attempt, assuming micro-motions at some faults of that area.

The observed pattern of uplift for the period 1997 to 2001 (Fig. 4) seems to be consistent with the theoretically estimated one (35-80mm), as predicted by the combined Mogi source and Fault modelling (Fig. 5), mostly at the central and western part of Nisyros. At the rest of the island the observed uplift is smaller by 20-25mm, as it is actually expected since the island's ground surface has the tendency to deflate since 1998 onwards.

Table 1. Parameters of Fault Dislocation for the Estimation of Deformation (Feigl & Dupre, 1999)

Fault No (Fig. 5)	Strike (a) (deg CW N)	Depth *d* (km)	Dip δ (deg)	U_1 (mm)	U_2 (mm)	U_3 (mm)	Length (km)	Width (km)
1	335.0	2.0	80.0	-80	-23	-33	3.0	2.03
2	67.0	0.4	70.0	25	-10	10	0.4	0.42
3	8.0	0.6	70.0	-54	-15	20	0.6	0.63
4	27.0	2.0	70.0	-50	-15	45	2.0	2.03
5	155.0	0.5	70.0	15	-10	18	0.5	0.53

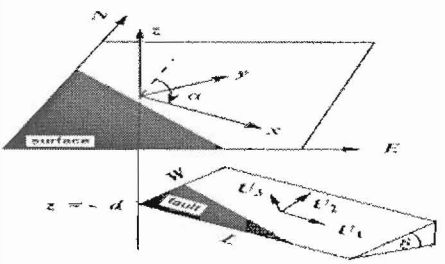

Figure 6. Diagrammatic Representation of Fault Parameters for the estimation of Deformation (after Feigl & Dupre, 1999).

3. Differential Interferometry (DInSAR)

Differential synthetic aperture radar interferometry (DInSAR) is the most interesting technique of SAR Interferometry (Massonnet and Rabaute, 1993) in the two-dimensional mapping of deformation with very high accuracy of mm to cm level. Differential radar interferometry was applied to study the regional deformation of the area in conjunction with the DGPS observations existed in the area since June 1997. The output of the DGPS results is used as control on the produced interferograms.

Suitable interferometric pairs of SAR images have been selected and presented in Table 2. The "two-pass differential interferometric method" or "DEM-elimination method" has been chosen, using two SAR images, to produce one interferogram. A second interferogram had to be created or synthesised to perform the differential analysis. The synthesized interferogram was generated from an existing digital elevation model (DEM) with pixel size 2 m and subsequently subtracted from the original interferogram. After removing all fringes which are related to ground elevation, only the fringes representing surface displacements remain. The phase differences, which remain as fringes in the differential interferogram, are the result of a range of changes of any displaced point

Table 2. Interferometric pairs

DATE	ORBIT	FRAME	PASS	SATELLITE	Bp (m)
22-MAY-1995	20135	2871	DESCENDING	ERS-1	
22-JAN-1996	23642	2871	DESCENDING	ERS-1	87
↕5 months gap					
11-JUN-1996	5973	2871	DESCENDING	ERS-2	
06-JUL-1999	22005	2871	DESCENDING	ERS-2	-45
↕5 months gap					
05-DEC-1999	24188	729	ASCENDING	ERS-2	
10-SEP-2000	28196	729	ASCENDING	ERS-2	-103

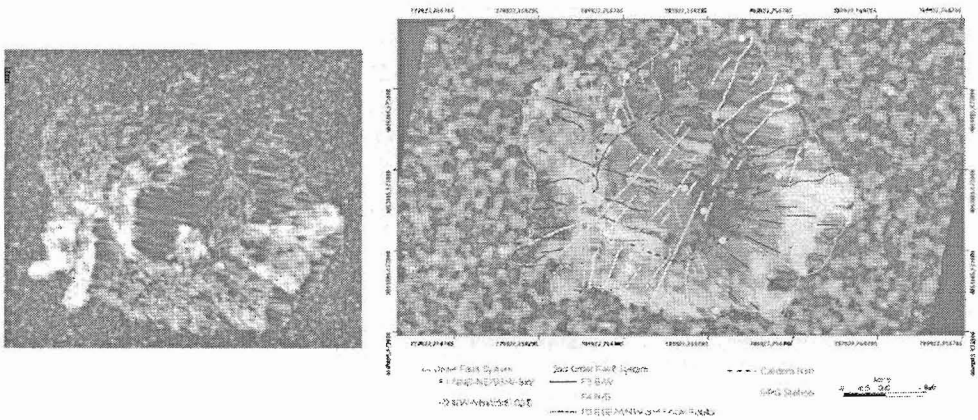

Figure 7. Coherence (left) and Differential Interferometric Image (right) of Nisyros Island (Magnitude & Phase) for the period 1995-1996. One fringe of deformation (28 mm) is represented by three colors (RGB).

on the ground from one interferogram to the next. In the differential interferogram, each fringe is directly related to the radar wavelength (56mm for ERS satellites) and represents a displacement relative to the satellite of only half the above wavelength (28mm). The detailed procedure for Nisyros DInSAR processing is described elsewhere (Pacharidis & Lagios 2001).

Figures 7, 8 & 9 present the interferograms for the three interferometric pairs, 1995-1996, 1996-1999, 1999-2000, respectively. Since the coherence characterizes the quality of the interferogram, the coherence map of the island for each period is also presented. In the coherence map, the brighter areas represent the area with good coherence, while the darker areas represent low coherence sections. In these interferograms it appears that the SE and SW part of the island have a better coherence, while its northern and most of the caldera area shows low coherence, losing thus information at these sections. This may happen due to the higher vegetation in the northern part, to the steep slopes of the Caldera rim, the cultivation in the northern part of the island and in the flat part

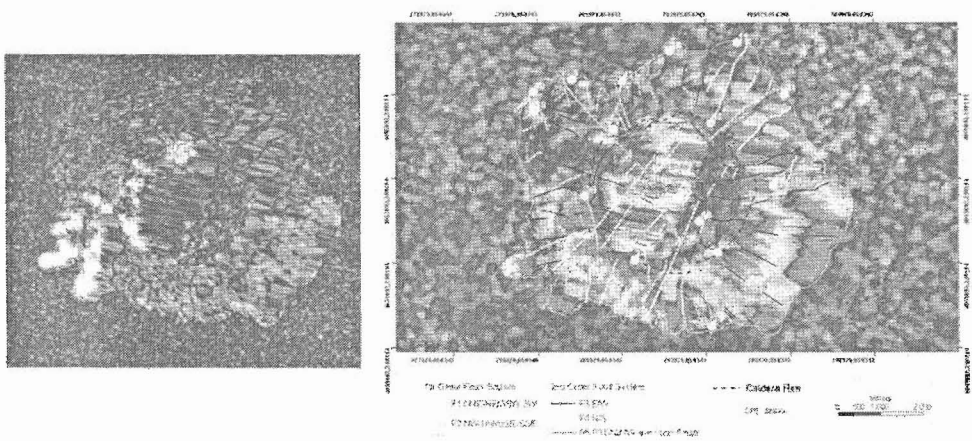

Figure 8. Coherence and Differential Interferometric Image of Nisyros Island for the period 1996-1999.

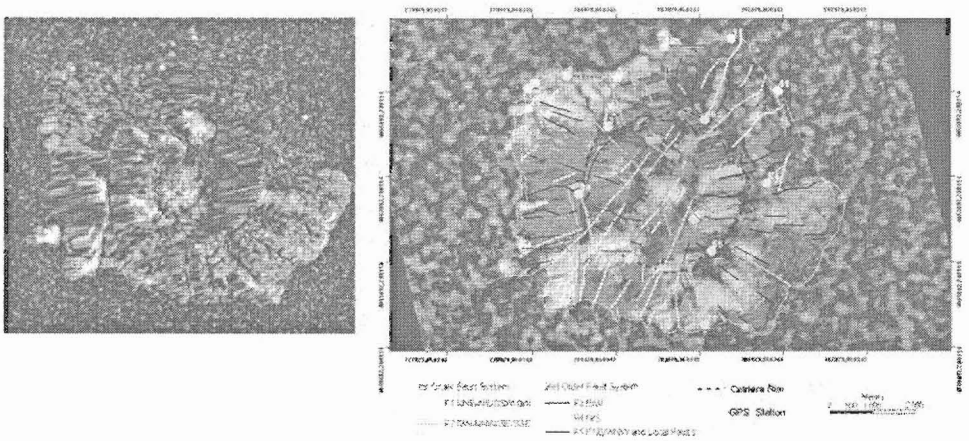

Figure 9. Coherence and Differential Interferometric Image of Nisyros Island for the period 1999-2000.

of the caldera, and also maybe due to the surface geology of the island which consists of andesites and dacites in the southern part, while, the northern part is covered mainly by unconsolidated pyroclastic material.

In the differential interferogram of the period 1995-1996 (Fig. 7), a major circular fringe covering most of the island, and a smaller one in the western part could be recognised. The coherence in these parts of the island is good. The rest of the image is covered by "rumor" or fringes related to the topography.

In the interferogram of the period 1996-1999 (Fig. 8), the coherence is low at the northern part and high at the SE and SW part of the island, while two quarter-circular shaped fringes in the SW part and one and a half fridges at the SE part are formed. A total displacement of about 56 mm along the slant range is observed for this time period, which covers the period of the highest seismic activity during 1996-1997. Finally, for the period 1999-2000 (Fig. 9), one fringe of surface deformation appears in the SE part of the island; there is also a possibility of another fringe in the central part of the island, having a different pattern from the previously described ones.

Summarizing for the three interferograms, a total number of four fringes of deformation can confidently be identified, which may be extended to five, if the last one of different pattern in the last interferogram is included, resulting thus in a total of 112-140 mm of ground deformation. In all interferograms, the phase increases from the inner to the outer part of the island, suggesting that in all cases the deformation is higher in the outer part. This seems to be consistent to the observed DGPS measurements (Fig. 4).

4. Discussion

The determined location of the Mogi source (Fig. 5) seems to almost coincide to where the two major faulting zones F1 and F2 are crossing, suggesting a weakening of the upper crustal layers in this area. The identified location and depth (7000 m) of the Mogi model is in agreement with previous results of other geophysical methods. Audio-Magnetotelluric (AMT) measurements in the Nisyros high enthalpy geothermal field (Lagios, 1991) indicated two conductive sources beneath about the centre of the island. These sources were interpreted as conductive bodies associated with the presence of the magma chamber (Dawes and Lagios, 1991). The deeper source inferred by the major axes of the MT polarisation ellipses in the period range of 0.1-0.01 Hz is situated almost on the junction of the two main faulting zones F1 and F2 (Fig. 2) at about the centre of the island, and at a depth of about 6-9 km, consistent to the identi-

fied Mogi model.

Detailed seismic tomographic studies (Makris and Chonia, 1999) in Nisyros and broader area clearly suggest a low velocity zone beneath Nisyros, associated with the geometry of a potential magma chamber at depths consistent to the location and depth of the Mogi model.

A possible emplacement of magma from deep crustal levels into a magma chamber at 7-8km depths has most probably been triggered by the 1995/96 intermediate to deep earthquakes of large magnitudes (Lagios et al., 1991), which led to a weakening of the crust. The replenishment of magma into a pre-existing magma chamber may also have caused changes in the thermal and pressure regime of the overlying hydrothermal system beneath Nisyros and the shallow fault systems. It reactivated older faults, (e.g. the fault passing through Mandraki), and thus producing tectonic micro-earthquakes in the upper crust. The random distribution of the microseismic foci (up to $M_s \sim 4$) during the seismic crisis 1996/97 around Nisyros, Yali and Strongyli, permits the interpretation of a magmatic origin micro-earthquakes. These seismic events may be generated by magma ascent through the crust opening fissures and plains through magma injection, volume changes of the magma during emplacement and cooling, as well as magma degassing accompanied by immediate volume expansion of the gas.

Acknowledgements

This project was financed by the EU IST-12310 project GEOWARN (www.geowarn.org).

References

Dawes, G.J.K. & Lagios, E. (1991). A Magnetotelluric Survey of the Nisyros Geothermal Field (Greece). *Geothermics*, 20/4, 225-235.

Feigl K. & Dupre E. (1999). RNGCHN: A program to calculate displacement components from dislocations in elastic half-space with applications for modelling geodetic measurements of crustal deformation. *Computers and Geosciences*, 25 (6), 695-704.

Gorceix, M.H. (1873a): Sur l'ıtat du volcan de Nisyros au mois de mars 1873. *C.R. Acad. Sci.* Paris 77, 597-601.

Gorceix, M.H. (1873b): Sur la ıcente ıruption de Nisyros. *C.R. Acad. Sci.* Paris 77, 1039.

Gorceix, M.H. (1873c): Sur l'ıruption boueuse de Nisyros. *C.R. Acad. Sci.* Paris 77, 1474-1477.

Ioannidis K. (1998). Nisyros Island: Observed damages to buildings in Mandraki. *Newsletter, European Center on Prevention and Forecasting of Earthquakes*, No 2, 33-35.

Jackson J.J. (1994). Active tectonics of the Aegean Region. Annual Rev. Earth Planet Sci., 22, 239-271.

Lagios, E. (2000): Intense crustal deformation rates on Nisyros Island (Greece), deduced from GPS studies, may foreshadow a forthcoming volcanic event. *Proc. 2nd Intern. Conf. On Earthquake Hazard and Seismic Risk Reduction (S. Balassanian et al, eds.)*, Kluwer Academic Publishers, p. 249-259.

Lagios E. (1991). Magnetotelluric study of the structure of the Nisyros Geothermal Field. *Bull. Geol. Soc. Greece*, 25/3, 393-407.

Lagios E., Dietrich, V., Stavrakakis G., Parcharidis I., Sakkas V., Vassilopoulou, S., 2001, Will Nisyros Volcano (GR) Become Active? Seismic Unrest and Crustal Deformation. *European Geologist*, 12, 44-50.

Lagios, E., Chailas, S., Giannopoulos, J. Sotiropoulos, P. (1998): Surveillance of Nisyros Volcano: Establishment and remeasurement of GPS and Radon Networks. *Bull. Geol. Soc. Greece*, vol. 32/4, 215-227.

Makris, J., Chonia, T. (1999): Active and Passive Seismic studies of Nisyros Volcano, East Aegean Sea. Proceedings of the 1999 CCSS Workshop held in Dublin, Ireland. *"Active and Passive Seismic Techniques Reviewed"*, Edts. A.W.Brian Jacob, Chr.J. Bean, Stephen T.F. Jacob, 9-12.

Massonnet, D., Rabaute, T. (1993): Radar interferometry: limits and potential, *IEEE Trans. Geosc. & Remote Sensing*, 31, 455-464.

Mogi, K. (1958): Relations between the eruptions of various volcanoes and the deformations of

ground surfaces around them. *Bull. Earthquake Res. Inst. Univ. Tokyo*, 36, 99-134.

Okada, Y., (1985): Surface deformation to shear and tensile faults in a half-space. *Bull. Seism. Soc. Am.*, 75, (4), 1135-1154.

Papanikolaou, D. & Lekkas, E., 1990. Geological structure and evolution of the Nisyros Volcano. *Bull. Geol. Soc. Greece*, XXV/1, 405-419.

Papanikolaou, D.J., Lekkas, E.L. & Sakelariou, D.T. (1991): Geological structure and evolution of Nisyros volcano. *Bull. Geol. Soc. Greece* 25/1, 405-419.

Parcharidis, I., & Lagios, E., 2001. Deformation in Nisyros Volcano (Greece) using Differential Radar interferometry. *Bull. Geol. Soc. Greece*, 1587-1594

Rothacher, M., Beutler, G., Gurtner, W., Brockmann, E., & Mervart, L. 1993. Bernese GPS Software Documentation version 3.4. Astronomical Institute, University of Berne, Switzerland

Sigmundsson, F. (1995): GPS Monitoring of Volcanic Deformation in Iceland. *Cahiers du Centre Europeen et de Seismologie*, Vol. 8, 79-98.

Sigmundsson, F., Einarsson, P., Bilham, R. (1992): Magma chamber deflation recorded by the Global Positioning System: The Hekla 1991 eruption. *Geophys. Res. Letters*, 19, 1483-1486.

Vougioukalakis, G., 1993. Volcanic stratigraphy and evolution of Nisyros Island. *Bull. Geol. Soc. Greece*, 28/2, 239-258

Zebker, H. and Goldstein, R. 1986. Topographic Mapping from Interferometric SAR Observations, *Journal of Geophysical Research*, Vol., 91, B5, 4993-4999.